

# Visualization of cargo concentration by COPII minimal machinery in a planar lipid membrane

Kazuhito V Tabata<sup>1</sup>, Ken Sato<sup>2,\*</sup>, Toru Ide<sup>3</sup>,  
Takayuki Nishizaka<sup>4</sup>, Akihiko Nakano<sup>5,6</sup>  
and Hiroyuki Noji<sup>1</sup>

<sup>1</sup>Department of Biomolecular Energetics, The Institute of Scientific and Industrial Research, Osaka University, Ibaraki, Osaka, Japan,

<sup>2</sup>Department of Life Sciences, Graduate School of Arts and Sciences, University of Tokyo, Meguro-ku, Tokyo, Japan, <sup>3</sup>Network Center for Molecular and System Life Sciences, Graduate School of Frontier Biosciences, Osaka University, Suita, Osaka, Japan, <sup>4</sup>Department of Physics, Gakushuin University, Toshima-ku, Tokyo, Japan, <sup>5</sup>Molecular Membrane Biology Laboratory, RIKEN Advanced Science Institute, Wako, Saitama, Japan and <sup>6</sup>Department of Biological Sciences, Graduate School of Science, University of Tokyo, Bunkyo-ku, Tokyo, Japan

**Selective protein export from the endoplasmic reticulum is mediated by COPII vesicles. Here, we investigated the dynamics of fluorescently labelled cargo and non-cargo proteins during COPII vesicle formation using single-molecule microscopy combined with an artificial planar lipid bilayer. Single-molecule analysis showed that the Sar1p–Sec23/24p-cargo complex, but not the Sar1p–Sec23/24p complex, undergoes partial dimerization before Sec13/31p recruitment. On addition of a complete COPII mixture, cargo molecules start to assemble into fluorescent spots and clusters followed by vesicle release from the planar membrane. We show that continuous GTPase cycles of Sar1p facilitate cargo concentration into COPII vesicle buds, and at the same time, non-cargo proteins are excluded from cargo clusters. We propose that the minimal set of COPII components is required not only to concentrate cargo molecules, but also to mediate exclusion of non-cargo proteins from the COPII vesicles.**

*The EMBO Journal* advance online publication, 17 September 2009; doi:10.1038/emboj.2009.269

*Subject Categories:* membranes & transport

*Keywords:* cargo packaging; COPII; transport vesicle; vesicle transport

## Introduction

Intracellular protein transport between the organelles of the secretory pathway is mediated by transport vesicles, which bud from a donor organelle and fuse with an appropriate acceptor membrane of a different compartment (Bonifacino and Glick, 2004). The formation of transport vesicles and sorting of cargo molecules into the emerging vesicles are mediated by coat protein complexes associated with the cytoplasmic face of the organelles (Kirchhausen, 2000;

Bonifacino and Lippincott-Schwartz, 2003). A common feature of transport vesicles is that most of them use small GTPases to regulate coat assembly at the donor membranes. The COPII coat is responsible for direct capture of transmembrane cargo proteins and for the physical deformation of the endoplasmic reticulum (ER) membrane that drives the formation of COPII vesicles in anterograde transport from the ER to the Golgi (Lee *et al.*, 2004; Sato and Nakano, 2007). COPII coat consists of the small GTPase Sar1p (Nakano and Muramatsu, 1989), the Sec23/24p complex, and the Sec13/31p complex that sequentially bind to the ER membrane (Barlowe *et al.*, 1994). COPII vesicle formation is initiated by GDP–GTP exchange on Sar1p catalysed by the transmembrane guanine nucleotide exchange factor Sec12p (Barlowe and Schekman, 1993). GTP binding triggers the exposure of the N-terminal amphipathic  $\alpha$ -helix element of Sar1p that inserts into the ER membrane (Huang *et al.*, 2001; Bi *et al.*, 2002). Membrane-bound Sar1p–GTP recruits the Sec23/24p complex by binding to the Sec23p portion (Bi *et al.*, 2002), and the cytoplasmically exposed signal of the transmembrane cargo is captured by direct contact with Sec24p (Miller *et al.*, 2003; Mossessova *et al.*, 2003) to form a prebudding complex (Kuehn *et al.*, 1998). The Sec23p subunit of the Sec23/24p complex is the GTPase-activating protein for Sar1p (Yoshihisa *et al.*, 1993) and therefore stimulates Sar1p GTP hydrolysis on binding to Sar1p, which leads to disassembly of the prebudding complex (Antonny *et al.*, 2001). However, the association of Sec23/24p on membranes can be maintained by interactions with cargo proteins and continual GTP loading of Sar1p by Sec12p (Futai *et al.*, 2004; Sato and Nakano, 2005). Subsequently, the prebudding complex is thought to be polymerized by the Sec13/31p complex to generate COPII vesicles. At the final stage of vesicle formation, the neck of a COPII vesicle bud is not likely to break spontaneously and the N-terminal amphipathic helix of Sar1p seems to have an active role in membrane fission (Bielli *et al.*, 2005; Lee *et al.*, 2005).

The molecular mechanisms of cargo sorting and transport carrier formation have been analysed in great detail mostly through *in vitro* reconstitution assays. COPII vesicles have been used as a model system to study the molecular mechanism of transport vesicle biogenesis as they can be generated from isolated organelles (Barlowe *et al.*, 1994), synthetic liposomes (Matsuoka *et al.*, 1998), and cargo-reconstituted proteoliposomes (Futai *et al.*, 2004; Sato and Nakano, 2004). However, those earlier *in vitro* vesicle budding assays were unable to track cargo molecules in the spatially and temporally resolved manner required to determine the number and density of cargo molecules encapsulated in each vesicle. As we reported earlier, a horizontal planar lipid bilayer reconstituted with transmembrane proteins can be easily and reproducibly formed across a small hole in a partition between two aqueous compartments (Ide and Yanagida, 1999; Ide *et al.*, 2002). We reconstituted fluorescently labelled

\*Corresponding author. Department of Life Sciences, Graduate School of Arts and Sciences, University of Tokyo, 3-8-1 Komaba, Meguro-ku, Tokyo 153-8902, Japan. Tel.: +81 3 5454 6749; Fax: +81 3 5454 6730; E-mail: kensato@bio.c.u-tokyo.ac.jp

Received: 5 June 2009; accepted: 17 August 2009

transmembrane cargo protein into the planar lipid bilayer together with Sec12p, and visualized the spatiotemporal dynamics of cargo molecules induced by the minimum

machinery required for COPII vesicle formation using a fluorescent microscope designed for single-molecule detection (Figure 1A). This system enables us to quantitatively

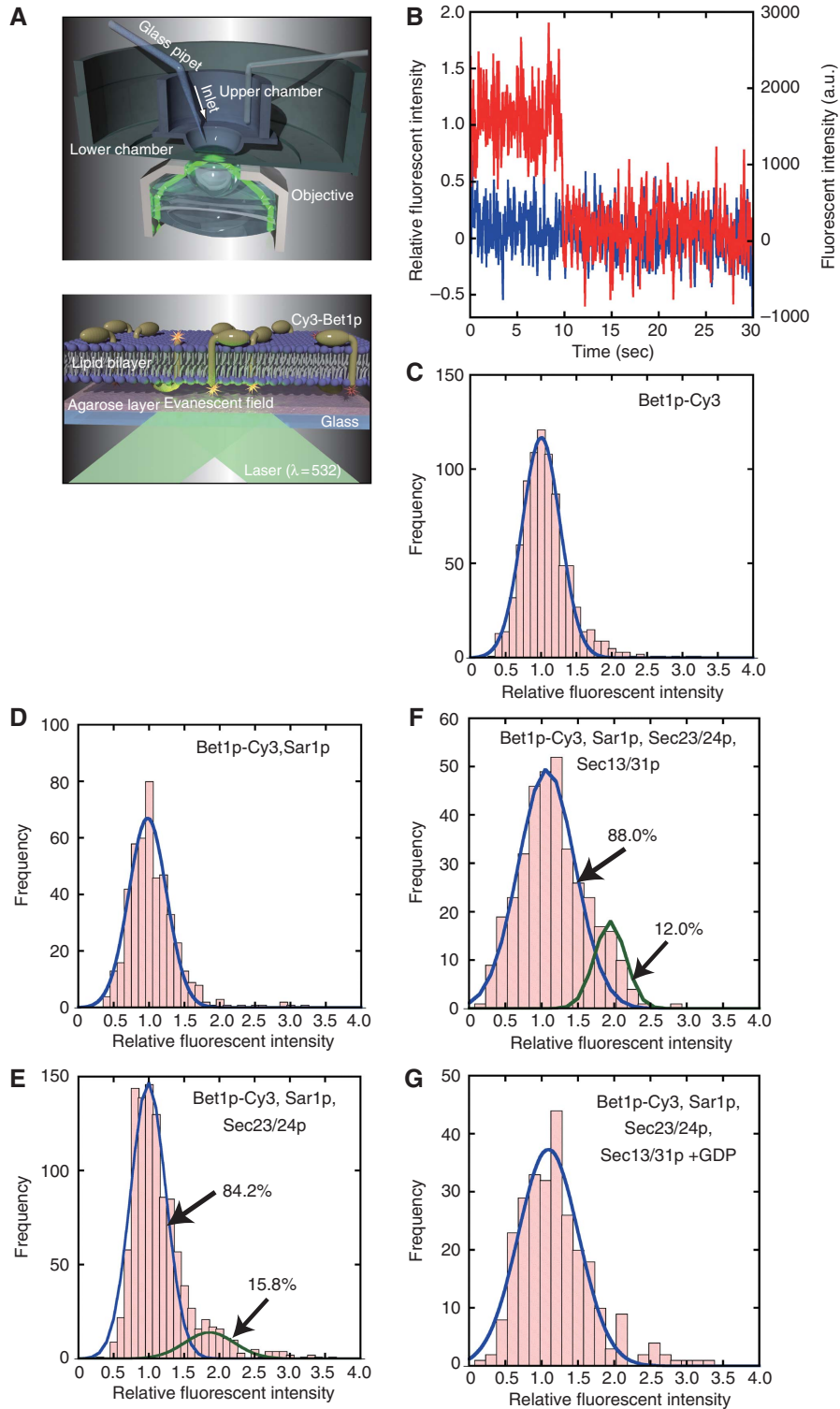


**Figure 1** Imaging of Bet1p-Cy3 molecules reconstituted in a planar lipid bilayer. (A) Overview of the horizontal planar lipid bilayer formation apparatus. The apparatus consists of two chambers. On the bottom of the upper chamber, a thin plastic film with a small hole (~100 μm) was attached and an artificial planar lipid bilayer was formed horizontally across the hole on an agarose-coated coverslip. The upper chamber could be moved vertically using a micromanipulator. (B) A typical fluorescent spot of Bet1p-Cy3 in the bilayer membrane was photobleached in a single step (red) to the background level (blue). (C-G) Distribution of the fluorescence intensity of Bet1p-Cy3 in the presence of the COPII component(s). To the bilayer membranes reconstituted with Bet1p-Cy3 (0.28 molecules μm<sup>-2</sup>) and Sec12Δlum (C) was added Sar1p (70 ng) (D), Sar1p (70 ng) and Sec23/24p (410 ng) (E), or Sar1p (70 ng), Sec23/24p (410 ng), and Sec13/31p (1.4 μg) (F) in molar excess of Bet1p-Cy3 in the presence of GTP, except for experiments in (G), in which GDP was added in place of GTP. Histograms of the fluorescence intensity were fit to either single or double Gaussian distributions (lines) and the percentages of fractions of each component are indicated (numbers).

resolve the assembly behaviour of cargo molecules in each step of the biochemically defined subreactions of COPII vesicle formation.

## Results

### **The behaviour of Bet1p molecules in the early stages of COPII vesicle formation**

We chose yeast ER–Golgi v-SNARE Bet1p as a model cargo for this study. As the wild-type yeast Bet1p has no cysteine, a cysteine addition to the C-terminal end allows Cy3-maleimide to be specifically attached so that a single Bet1p molecule possesses a single molecule of Cy3 (Bet1p–Cy3). Bet1p–Cy3 was reconstituted in a planar lipid bilayer with a major–minor mix formulation (Matsuoka *et al*, 1998) optimized for COPII assembly. Approximately 90% of the N-terminal elements of the reconstituted Bet1p–Cy3 were oriented towards the upper surface of the bilayer membrane (Sato and Nakano, 2005). When Bet1p–Cy3 was visualized with evanescent field illumination, each dot moved in the membrane laterally with a diffusion coefficient ( $D$ ) of  $D = 4.5 \pm 2.0 \mu\text{m}^2 \text{s}^{-1}$ , indicating that Bet1p–Cy3 molecules were able to move freely within the membrane, even though the membrane was in contact with the agarose layer on the coverslip. We examined the fluorescent intensity and photobleaching characteristics of every dot to clarify whether the single fluorescent dots in the membrane represented a single Bet1p molecule. Time-dependent changes in fluorescent intensity for individual dots in the membrane showed single-step photobleaching, which is characteristic of single fluorophores (Figure 1B). The distribution of the fluorescent intensities of the dots fit well with a single Gaussian distribution with a peak intensity similar to that of the step size for photobleaching (Figure 1C). These results indicated that Bet1p–Cy3 alone existed as a monomer in the bilayer membrane.

We next examined the behaviour of Bet1p molecules in the presence of a subset of COPII components. The binding of Sar1p to Bet1p has been shown to precede recruitment of Sec23/24p (Springer and Schekman, 1998). We reconstituted both Bet1p–Cy3 and Sec12 $\Delta$ lum (Sec12p without its luminal domain, but containing the transmembrane region) (Sato and Nakano, 2005) in the bilayer membrane and added Sar1p and Sec23/24p in molar excess of Bet1p–Cy3 to the membrane in the presence of GTP. The diffusion coefficient of Bet1p–Cy3 was decreased by the addition of Sar1p ( $D = 2.6 \pm 1.4 \mu\text{m}^2 \text{s}^{-1}$ ) or by both Sar1p and Sec23/24p ( $D = 2.8 \pm 1.8 \mu\text{m}^2 \text{s}^{-1}$ ), most likely as a result of the association of Bet1p–Cy3 with Sar1p and Sec23/24p. The distribution of the fluorescence intensity of Bet1p–Cy3 in the presence of Sar1p–GTP showed a single peak, which fit well with a single Gaussian distribution (Figure 1D), and the fluorescence intensity from each Bet1p–Cy3 decayed in a single step (data not shown), suggesting that the Bet1p molecules bound to Sar1p existed as monomers. In contrast, the distribution of the fluorescence intensity of Bet1p–Cy3 in the presence of both Sar1p–GTP and Sec23/24p was fitted to a sum of two Gaussian distribution functions (Figure 1E). The fluorescent dots in the first component showed single-step-bleaching characteristics, suggesting that the first component contained single Bet1p–Cy3 molecules (data not shown). The second component (15.8% of the fraction), which emitted a signal twice as intense as the first component, should

represent dots containing two Bet1p–Cy3 molecules. This component most likely represents self-dimerization of the prebudding complexes rather than two Bet1p–Cy3 molecules captured within a single Sec23/24p coat, because Sec23/24p has been shown to be associated with a single Sar1p and Bet1p (Bi *et al*, 2002; Mossessova *et al*, 2003). We also visualized prebudding complexes labelled with Sar1p–Cy3 (Supplementary Figure S1). A portion of Sar1p–Cy3 dots also shifted from the monomeric region to the dimeric region on the addition of Sec23/24p in the presence of nonlabelled Bet1p. In contrast, Sar1p–Cy3 that associated with Sec23/24p in the absence of Bet1p remained a monomer. These results suggest that partial dimerization occurs only between prebudding complexes but not within Sar1p–Sec23/24p complexes.

### **Visualization of cargo recruitment into forming COPII vesicles and vesicle release from the membrane**

We next traced Bet1p–Cy3 molecules in the presence of the complete set of COPII components to visualize cargo recruitment into forming COPII vesicles followed by release of the vesicles from the planar bilayer membrane. Bet1p–Cy3 accumulation into nascent COPII vesicles should be observed as a formation of spots with increased fluorescence intensity. In addition, as the evanescent field illumination images only those fluorescently labelled molecules within  $\sim 150$  nm above the surface of the coverslip, the disappearance of these fluorescent spots should represent the release of COPII vesicles away from the membrane. On addition of COPII components, however, the intensity distribution of the resulting spots showed that most of these spots contained less than two molecules, whereas Bet1p–Cy3 remained as a monomer with GDP (Figures 1F and G; Supplementary Movie S1). We also found that the accumulation of such fluorescent spots in the presence of the complete COPII coat was also accompanied by a constraint in their lateral mobility. These results suggest that the Sec13/31p-driven prebudding complex assembly is extremely inefficient under this condition. One possible explanation for this is that the loss of lateral mobility of prebudding complexes, as observed in Supplementary Movie S1, could limit the potential for Sec13/31p-mediated clustering. Alternatively, the interaction between the bilayer membrane and the agarose layer on the coverslip limited spherical polymerization of the prebudding complexes. To overcome this problem, the upper chamber was placed upward from the coverslip, where the distance between the bilayer and the coverslip was about 10–20  $\mu\text{m}$ , so as to position both sides of the membrane in an aqueous environment (Figure 2A). Under this condition, we acquired video images of the fluorescence from the membrane with epifluorescence illumination instead of evanescent field illumination. When COPII components were added onto the membrane, Bet1p–Cy3 was found to accumulate into mobile fluorescent spots with increased fluorescence intensity, followed by the formation of clusters in the membrane (Figure 2A; Supplementary Movie S2). The dynamics observed here confirmed the widely accepted hypothesis that the prebudding complexes are clustered by Sec13/31p.

To ensure that the bilayer membrane with this setting can support COPII vesicle generation, a complete set of COPII components was added to the lower chamber to induce vesicle budding in a downward direction towards the surface

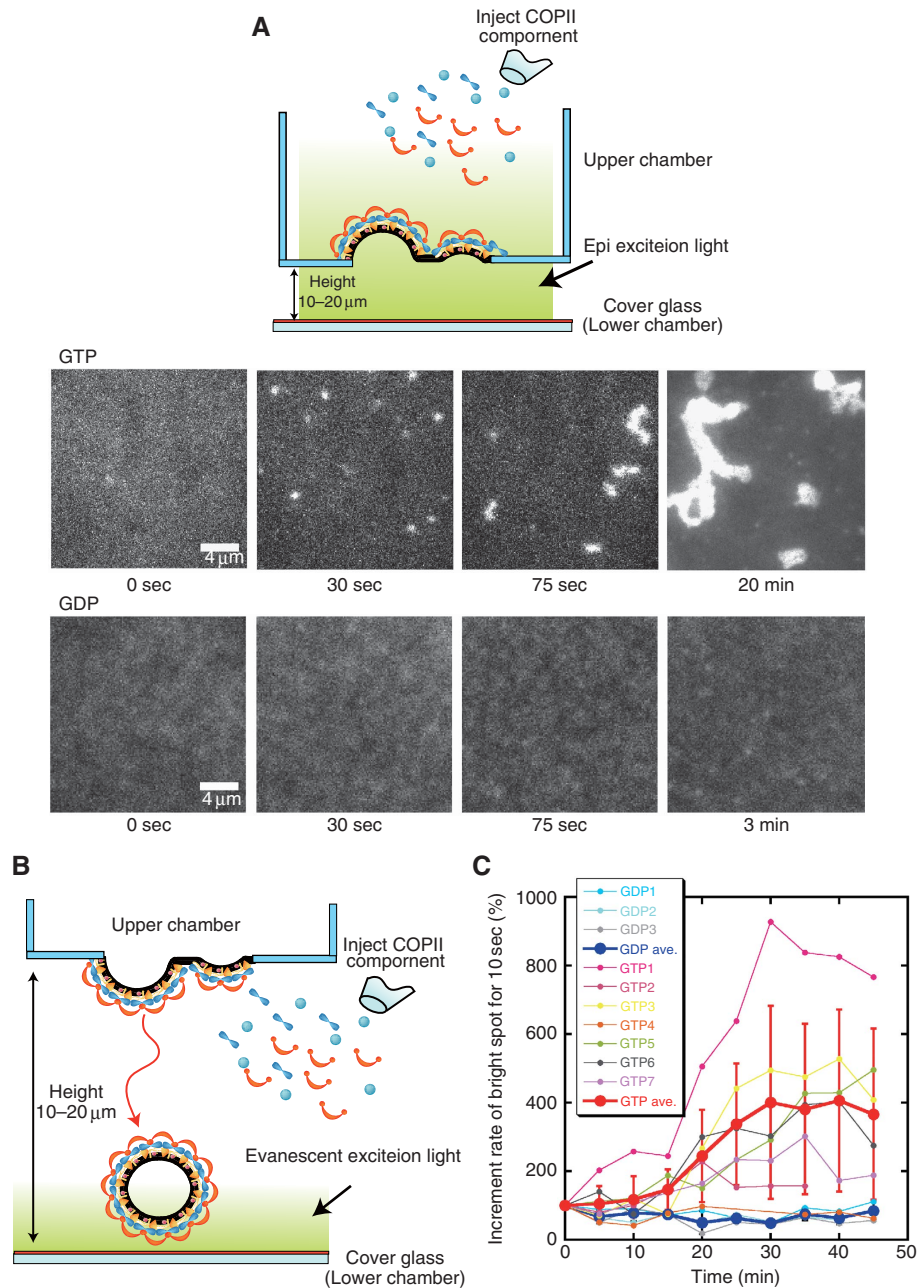


**Figure 2** Clustering of Bet1p-Cy3 molecules and downward COPII vesicle budding with the bilayer membrane formed in an aqueous environment. **(A)** Sequential images of the Bet1p-Cy3 clustering in the bilayer membrane (Supplementary Movie S2 online). Sar1p (70 ng), Sec23/24p (410 ng), and Sec13/31p (1.4  $\mu\text{g}$ ) were added to the bilayer membrane reconstituted with Bet1p-Cy3 (95.6 molecules  $\mu\text{m}^{-2}$ ) and Sec12 $\Delta$ lum at  $t = 0$  s in the presence of GTP or GDP as illustrated in the upper panel. Epifluorescence images were taken with exposure times of 66 ms. **(B)** Schematic illustration of downward COPII vesicle budding. **(C)** Time course of the increase in the number of fluorescent particles that appeared on the coverslip after the addition of the COPII components. Each thin trace corresponds to an individual experiment. The numbers of fluorescent particles were normalized so that the initial number of fluorescent particles on the coverslip was 100%. Thick traces with standard error deviations represent the averages of all thin traces.

of the coverslip, and the fluorescence signals that appeared on the coverslip surface were detected using evanescent field illumination (Figure 2B). As only  $\sim 10\%$  of the N-terminal elements of the reconstituted Bet1p were oriented towards the coverslip, we used Bet1p-4Cy3 at a concentration 300-fold higher than that used in Figure 1 to increase the signal intensity for these experiments. After 30 min incubation, small fluorescent particles undergoing rapid Brownian motion were observed on the surface of the coverslip, whereas

no signals were observed immediately after COPII addition (Supplementary Movie S3). These fluorescent particles may represent the COPII vesicles incorporated with Bet1p-4Cy3. By counting the number of fluorescent particles at different time points after the addition of COPII components, we obtained a time course of COPII vesicle production (Figure 2C). The particle number increased in proportion to the incubation time and reached a plateau after about 30 min of incubation. Fluorescent signals were infrequently observed

in the presence of GDP, indicating specific accumulation of vesicle formation. We conclude that the COPII components can generate COPII vesicles from the bilayer membrane under this condition.

### ***Incorporation of Bet1p molecules into a COPII vesicle bud is saturable***

To quantify the number of Bet1p molecules in a COPII vesicle bud immediately before the vesicle pinch-off, we needed to arrest the vesicle release from the membrane. To achieve this, we used a thick planar membrane. The planar bilayers of physiological thickness used in Figures 1 and 2 were formed with lipids dissolved in squalene (8.4 nm thickness). As the molecular environment between the monolayers in a bilayer changes with the solvent, the thickness of the planar bilayer increases approximately two-fold when decane is substituted for squalene (13.6 nm thickness) (data not shown). Bet1p-Cy3 reconstituted in the thick membrane behaved similarly to that shown in Figures 1 and 2A; that is, partial dimerization of prebudding complexes (data not shown) followed by accumulation into fluorescent spots (Supplementary Movie S4) except for the vesicle pinch-off as observed in Figure 2C (data not shown). Thus, the COPII components can collect cargo molecules in the thick membrane, but cannot induce vesicle pinch-off, possibly because of the membrane thickness (Supplementary Figure S2). To determine the number of Bet1p-Cy3 molecules contained in each COPII bud, we first acquired fluorescent spots in the thick membrane by the addition of the COPII components, and then the upper chamber was positioned down so that the membrane was attached to the coverslip. This procedure restricted the diffusion movements of only the assembled Bet1p-Cy3 in the membrane, but not those of monomeric Bet1p-Cy3 and the prebudding complex. Owing to the interaction between the membrane and the agarose layer, visualization of only the assembled Bet1p-Cy3 as immobile fluorescent spots became possible. Inspection of the fluorescent image arising from the presence of complete COPII components and GTP showed that the small fluorescent spots were scattered among several large asymmetric aggregates (Figure 3A, upper panel). According to their size, these aggregates are likely to correspond to the fluorescent clusters observed in Supplementary Movies S2 and S4, whereas the small spots are not visible in the movies because of rapid lateral diffusion. The distribution of the small spots appears relatively evenly spaced, which is similar to the results of a computational model for the process of COPII assembly (Heinzer *et al*, 2008). We selected these small spots, and the distribution of fluorescence intensity was analysed under several different concentrations of Bet1p-Cy3 in the membrane (Figure 3B, left panel). In all cases, the fluorescence intensity showed a single maximum. When the mean value of the fluorescence intensity was plotted against the Bet1p-Cy3 concentration, the fluorescence intensity increased in proportion to the concentration of Bet1p-Cy3 in the membrane and reached a plateau (Figure 3C). These results indicate that these small spots consisted of uniformly assembled Bet1p-Cy3 and that the incorporation of Bet1p-Cy3 into the spots is saturable. The saturation number of Bet1p-Cy3 molecules per spot was estimated to be about 70 on the basis of fluorescent intensity. On the basis of recent structural data on the cuboctahedral or icosidodecahedral cage assembled from Sec13/31p (Stagg *et al*, 2006, 2008), and

because Bet1p and Sec24p form a 1:1 complex (Mossessova *et al*, 2003), the theoretical maximum number of Bet1p molecules that can be captured by Sec23/24p into a single COPII vesicle is calculated to be 48 or 120. This value is close to the estimated saturation number of Bet1p-Cy3 in each spot. Therefore, it is likely that these small spots correspond to the structures of the COPII vesicle buds immediately before vesicle pinch-off. An important question is whether the large aggregates observed among the small spots were also active in vesicle generation, but it was not clear because of the difficulty in resolving the movement of individual COPII vesicles away from the membrane with our detection system.

### ***Sar1p GTPase cycles are required for efficient cargo recruitment into COPII vesicle buds***

Although Sar1p GTP hydrolysis is dispensable for COPII vesicle formation (Barlowe *et al*, 1994), we have shown earlier that Sar1p GTPase cycles selectively dissociate Sec23/24p molecules that are bound to anionic phospholipids, but not those associated with cargo proteins, which promotes cargo concentration (Sato and Nakano, 2005). To directly observe the effect of GTP hydrolysis on cargo concentration into the nascent COPII vesicle, we also investigated Bet1p-Cy3 assembly in the presence of a nonhydrolysable GTP analog, GMP-PNP, in the same manner as described for the measurement with GTP (Figure 3A, lower panel and , right panel). On addition of COPII components in the presence of GMP-PNP, fluorescent spots as well as large aggregates were monitored. However, the fluorescence intensity of spots and aggregates was significantly lower than that observed with GTP, and the images were associated with high background fluorescence (Figure 3C). These results indicate that cargo recruitment into nascent vesicles is inefficient in the absence of Sar1p GTPase cycles, and that significant amounts of Bet1p-Cy3 molecules remain outside the spots and aggregates. Moreover, the sizes of the large aggregates induced by GMP-PNP were similar to those of GTP, but displayed a speckled fluorescent pattern. As Sec23/24p also binds to anionic phospholipids in the membrane, cargo is not a requisite for membrane recruitment for Sec23/24p (Matsuoka *et al*, 1998). Thus, the presence of GMP-PNP results in the generation of stable complexes of both the Sar1p-Sec23/24p-cargo and Sar1p-Sec23/24p form. Therefore, the observed speckled aggregates, most likely representing these two forms of prebudding complexes, are clustered by Sec13/31p. These findings confirm the idea that the GTPase cycles of Sar1p are required for efficient cargo concentration into COPII vesicles.

### ***COPII minimal machinery is able to exclude non-cargo proteins form cargo clusters***

It is now quite evident that most transmembrane cargo molecules are actively sorted into the COPII vesicles by direct interactions with the coat proteins, whereas transmembrane ER-resident proteins can be retained in the ER either by static retention or by continuous signal-mediated retrieval from post-ER compartments (Sato and Nakano, 2007). Although transmembrane ER-resident proteins that have accidentally escaped by bulk flow are retrieved by COPI-coated retrograde vesicles, many ER-resident proteins seem to avoid bulk flow by static retention mechanisms that exclude them from entering COPII vesicles (Bonifacino and Glick, 2004; Lee

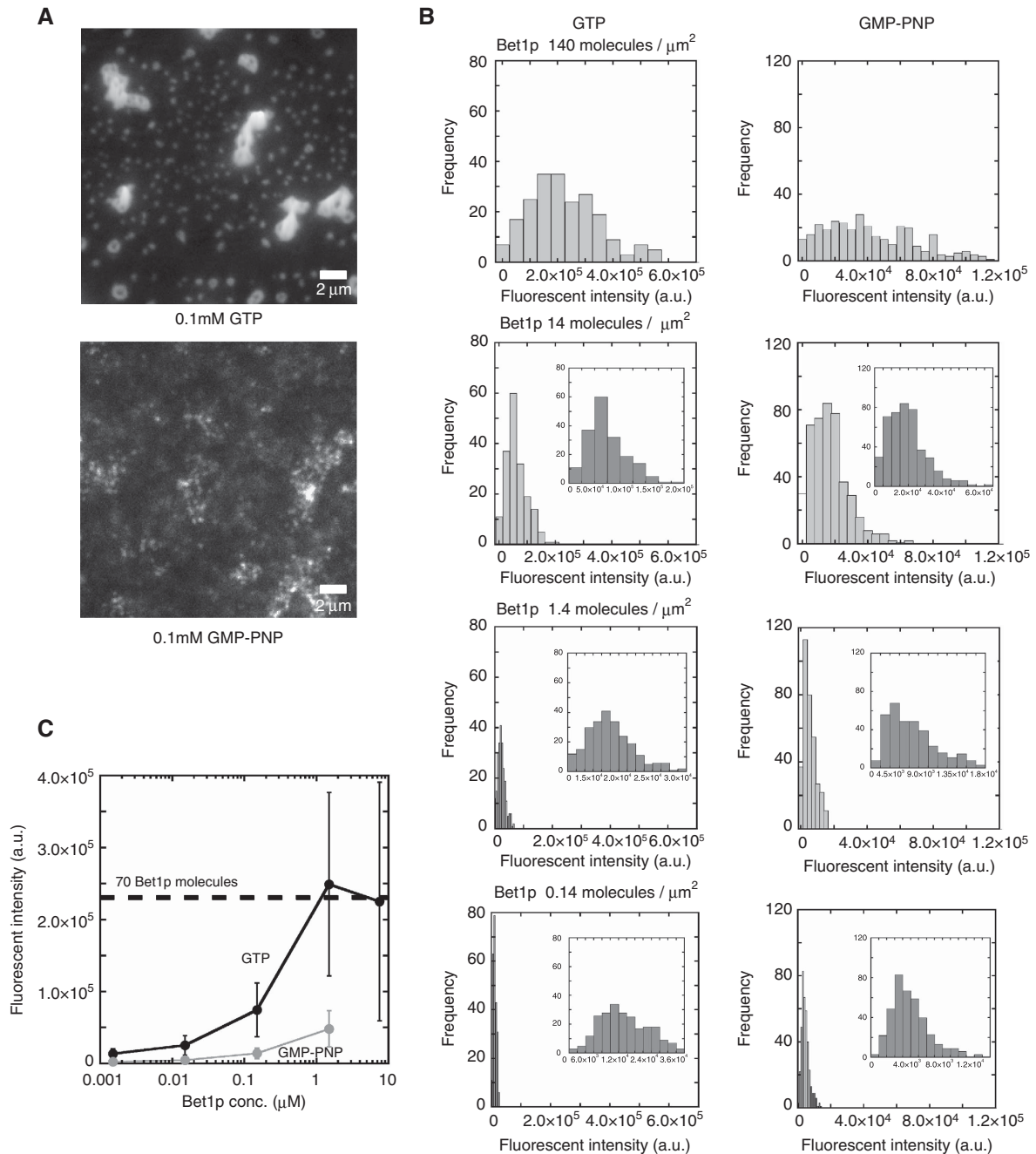


**Figure 3** COPII-induced Bet1p-Cy3 assembly in the decane bilayer membrane. **(A)** COPII components (70 ng Sar1p, 410 ng Sec23/24p, and 1.4  $\mu\text{g}$  Sec13/31p) were added from the upper chamber to the decane bilayer membrane formed in an aqueous environment and fluorescent spots were acquired (as shown in Supplementary Movie S4 online) in the presence of GTP (upper panel) or GMP-PNP (lower panel). The bilayer membrane was then attached to the coverslip. Fluorescent images were taken under evanescent field illumination. **(B)** Distribution of the fluorescence intensity of the small spots observed in **(A)** under different concentrations of Bet1p-Cy3 in the membrane. Insets show the same histograms plotted with a narrower bin size. **(C)** A correlation plot of the Bet1p-Cy3 concentration versus the mean fluorescent intensity of the fractions obtained from **(B)**.

*et al*, 2004). However, no components have been so far identified that are required for static ER retention.

To investigate whether the minimal set of COPII components can mediate exclusion of ER-resident proteins from COPII vesicles, we further studied the dynamics of fluorescently labelled ‘non-cargo’ proteins together with the dynamics of Bet1p-Cy3 during cargo assembly mediated by COPII components. For these experiments, we used ATTO647N-labelled MBP-Ufe1p (Sato and Nakano, 2004)

(Ufe1p-ATTO647N), a model for resident ER proteins. Both Bet1p-Cy3 and Ufe1p-ATTO647N were reconstituted into the bilayer membrane together with Sec12 $\Delta$ lum and we analysed their mutual localization in the presence of the COPII components. Fluorescence signals representing Ufe1p-ATTO647N and Bet1p-Cy3 molecules excited at each wavelength are shown in Figure 4A. In a control experiment with GDP, Ufe1p-ATTO647N and Bet1p-Cy3 exhibited equal mixing of ATTO647N and Cy3 fluorescence, indicating that these

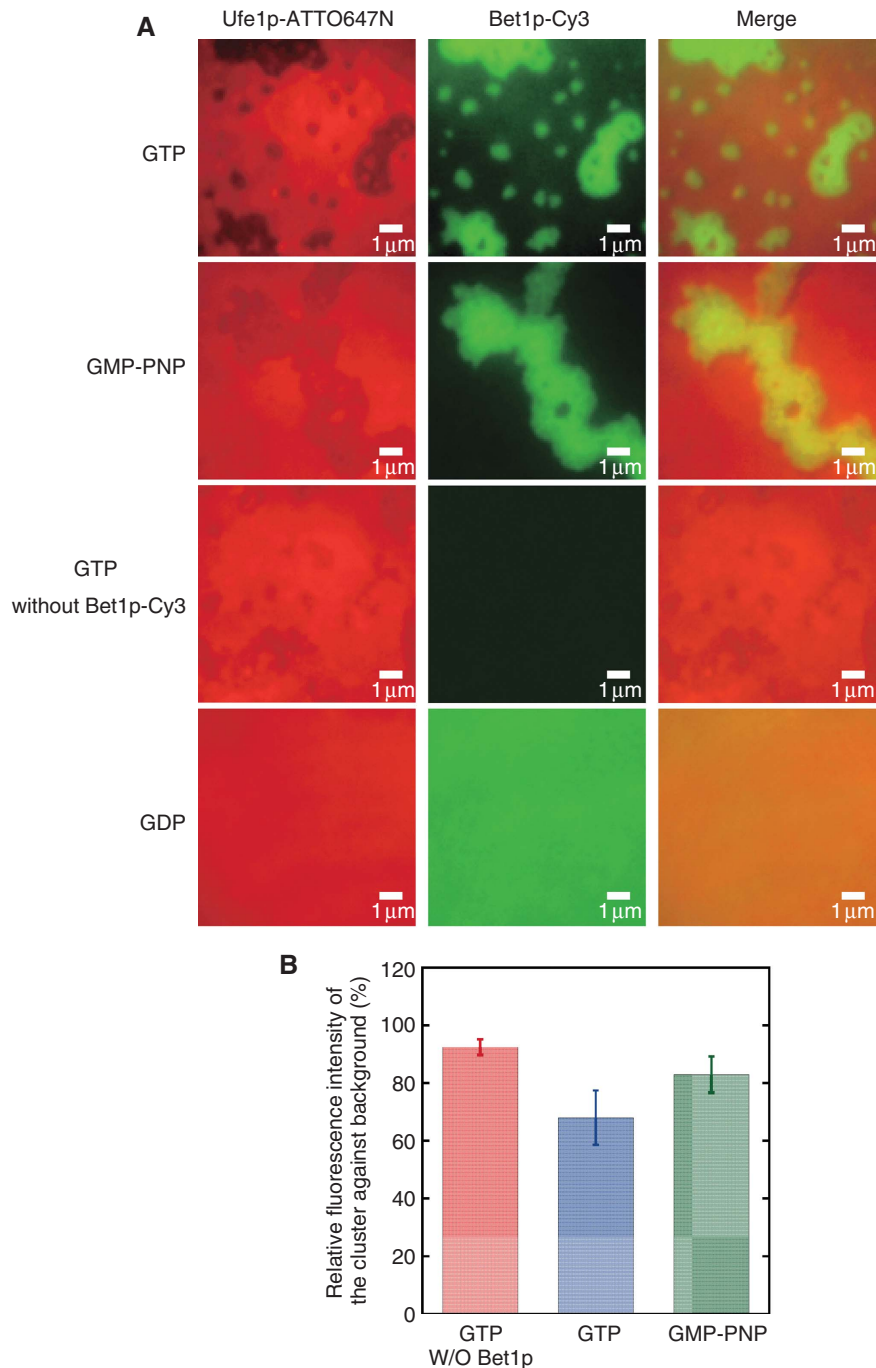


**Figure 4** The mutual localization of Ufe1p-ATTO647N and Bet1p-Cy3 in the presence of the COPII components. (A) Sar1p (70 ng), Sec23/24p (410 ng), and Sec13/31p (1.4  $\mu$ g) were added from the upper chamber to the decane bilayer membrane (formed in an aqueous environment) reconstituted with Ufe1p-ATTO647N (41.3 molecules  $\mu$ m<sup>-2</sup>), Bet1p-Cy3 (113.1 molecules  $\mu$ m<sup>-2</sup>), and Sec12 $\Delta$ lum molecules in the presence of GTP or GMP-PNP. Bet1p-Cy3 was omitted in some cases. The following procedures were the same as those for Figure 3A. ATTO647N (left) and Cy3 (centre) fluorescence channels, and merged image (right) are shown. ATTO647N and Cy3 fluorescence is shown in red and green, respectively. (B) The relative density of Ufe1p-ATTO647N in the large clusters compared to that outside the cluster.

molecules were randomly distributed relative to one another. However, when Ufe1p-ATTO647N molecules were visualized in the ATTO647N channel, the addition of the COPII components with GTP yielded large clusters observed as dark contrasting regions that were relatively devoid of fluorescent signals compared with the background (Figure 4A). These clusters are likely to represent COPII-mediated Bet1p-Cy3 clusters that are segregated from Ufe1p-ATTO647N because (1)

as apparent from a merged image, such regions overlapped to a great extent with the distribution of Bet1p-Cy3 clusters observed in the Cy3 channel and (2) such dark contrasting regions were not observed in the absence of Bet1p (Figure 4A). Without exclusion mechanisms, transmembrane proteins without export signals should be neither enriched nor depleted in Bet1p clusters, but the density of Ufe1p-ATTO647N included in Bet1p clusters was significantly

lower than that observed outside the clusters (68.0% of background fluorescence) (Figure 4B). Furthermore, the exclusion was less effective (83.0% of background fluorescence) in the presence of GMP-PNP. These results show that exclusion of non-cargo proteins from cargo clusters is at least partly mediated by the COPII minimal machinery, and that the process of exclusion requires Sar1p GTPase cycles. We further traced Cy3-labelled MBP-Ufe1p (Ufe1p-Cy3) co-reconstituted with nonlabelled Bet1p and Sec12 $\Delta$ lum in the presence of the COPII components, as shown in Supplementary Figure S3. The addition of the COPII components yielded large clusters observed as dark contrasting regions that were relatively low levels of fluorescent signals (Supplementary Figure S3A), as also observed in Figure 4A. These are likely to represent unlabelled Bet1p clusters that are segregated from Ufe1p-Cy3, because such regions were not observed in the absence of Bet1p (Supplementary Figure S3B).

## Discussion

We described quantitative, real-time imaging approaches to observe at the single-molecule level, the behaviour of cargo molecules during transport vesicle formation. In contrast to classical *in vitro* systems, which only monitor the ensemble average, our system provides a rigorous means to measure and visualize the response of individual molecules in the membrane undergoing transport vesicle formation.

Single-molecule detection showed that the prebudding complex undergoes partial dimerization in the membrane before Sec13/31p recruitment (Figure 1E). This property has not been detected earlier by using biochemical methods because only traces of the prebudding complex (<3%) can be retained in detergent solution (Kuehn *et al*, 1998). Although our measurements showed a relatively weak dimerization property (15.8%) of prebudding complexes, this lower dimerization efficiency might be due to the low concentration of Bet1p-Cy3 within the planar bilayer membrane (0.28 molecules  $\mu\text{m}^{-2}$ ), which may be well below the physiological concentration. However, this concentration is the maximum possible for resolving each fluorescent spot in the membrane. It can therefore be expected that efficient dimerization occurs under more physiologically relevant cargo concentrations. It remains to be determined which component of the prebudding complex provides an interface for dimerization. We also showed that the inclusion of a cargo molecule in the Sar1p-Sec23/24p complex was responsible for the partial dimerization of this complex (Supplementary Figure S1). One possibility is that the preformed prebudding complex dimer in the membrane provides a structural scaffold for Sec13/31p recruitment advantageous for assembly into the COPII cage, ensuring that only Sar1p-Sec23/24p-cargo complexes, but not Sar1p-Sec23/24p complexes, are efficiently assembled into the COPII cage. Recent *in vivo* data show that budding profiles can be seen on the ER membrane in the absence of functional coupling of Sec13/31p to the prebudding complex, and certain cargo molecules are being properly sorted to these sites (Fromme *et al*, 2007; Townley *et al*, 2008). These observations suggest that the prebudding complex is capable of clustering with each other and is sufficient to generate membrane curvature. However, we could not observe multimeric self-assembly of the prebudding complex in the absence of Sec13/31p. Thus,

these properties are likely to lie in other factors that modulate COPII-dependent budding, which could include Sec16p that has been shown to participate in COPII assembly (Gimeno *et al*, 1996; Supek *et al*, 2002). It is also possible that only a single kind of cargo *in vitro* is unable to induce such properties and the presence of prebudding complexes including a variety of cargo proteins may be required for the generation and/or stabilization of membrane curvature.

There is an earlier study showing that GTP hydrolysis is not required for COPII vesicle budding and vesicle pinch-off from microsomes, and the study also showed a similar efficiency of packaging of cargo proteins into COPII vesicles in incubations containing GTP or GMP-PNP with saturate amount of COPII proteins (Barlowe *et al*, 1994). However, as the microsome-based *in vitro* budding assay had difficulties with estimating the number of released vesicles, it was not clear whether the same number of COPII vesicles was produced by GTP and GMP-PNP. It is possible that GTP generates a small number of COPII vesicles but with high cargo density, whereas GMP-PNP produces a large number of COPII vesicles but with low cargo density. A major advantage of our system is that it can estimate the number of molecules contained in each vesicle bud formed in the membrane. We showed that the incorporation of Bet1p-Cy3 into COPII vesicle buds was saturable within the range of the predicted total number of coat proteins present on a single COPII vesicle (Figure 3C). If we assume a binding stoichiometry between coat and cargo of 1:1, our results are consistent with the widely accepted proposal that the maximum number of cargo molecules that can be loaded into a single vesicle is limited to the number of coat proteins on the vesicle surface. It was shown earlier that COPII vesicle formation can be minimally reconstituted using Sec23/24p, Sec13/31p, and GTP-locked Sar1p with cargo-reconstituted proteoliposomes (Sato and Nakano, 2004). In these experiments, however, the efficiency of cargo sorting was not comparable to that which can be achieved with intact ER membranes and purified COPII components in the presence of GTP. This was probably partly because of the lack of GTP hydrolysis, because the experiments in this study also clearly demonstrated that Sar1p GTPase cycles contribute to a higher efficiency of cargo sorting into COPII vesicles (Figure 3). These findings are consistent with the requirements for Sar1 GTPase activity in the concentration of cargo in living cells (Stephens and Pepperkok, 2004).

In earlier work on the reconstitution of COPII assembly on synthetic liposomes, COPII-coated buds but few if any free vesicles form in incubations containing GTP, COPII proteins, and the cytoplasmic domain of Sec12p (Futai *et al*, 2004). Our results provide evidence that artificial lipid bilayers reconstituted with Bet1p and Sec12p produce free vesicles in the presence of COPII components with GTP (Figure 2B). The difference between the two observations is the presence of embedded cargo and Sec12p. It is probable that cargo in general promotes membrane fission, or the presence of embedded Sec12p in the membrane might be necessary for vesicle pinch-off. For comparison, the Bet1p and COPII concentrations used in this study (0.28–140 copies of Bet1p per  $\mu\text{m}^{-2}$  and approximately 10 nM of each COPII component) were much lower than those used in classical *in vitro* assays (Sato and Nakano, 2004) using proteoliposomes and COPII proteins ( $\sim 4000$  copies of Bet1p per  $\mu\text{m}^{-2}$  and about 600 nM of each COPII coat component).



Although cargo packaging into transport vesicles is generally signal mediated and involves direct or indirect interactions between the coat proteins and cargo molecules, ER-resident proteins are regulated to localize to the ER by two mechanisms: retrieval and retention. In contrast to our detailed knowledge on the retrieval phenomena that operate within the vesicular transport pathway to counteract escape of proteins from their resident compartment, it has been more difficult to clarify the static retention mechanisms that underlie exclusion of resident proteins from transport vesicles. As a first step towards the biochemical characterization of static ER retention mechanisms, we investigated the dynamics of non-cargo proteins to test whether the COPII components are involved in this process. We showed that the core COPII machinery alone was able to efficiently exclude non-cargo proteins from Bet1p cargo clusters (Figure 4). Although it has been considered that a mechanism based on recognition between ER exit signals and COPII components is less likely to underlie cargo exclusion events, our findings show for the first time that the exclusion of non-cargo proteins is at least partly driven by the minimal COPII machinery. This leaves open the question as to how ER-resident proteins are actively prevented from entering the COPII vesicles. One possible model is that prebudding complexes may sterically exclude non-cargo proteins that should not belong to the vesicle. As Sar1p–Sec23/24p is suggested to interact closely with the membrane (Bi *et al*, 2002), such areas should be devoid of non-cargo proteins. Moreover, 48 copies of the Sar1p–Sec23/24p complex are estimated to cover as much as 80% of the surface area of a COPII vesicle (Fath *et al*, 2007), and the additional area would be occupied by the cytoplasmic regions of transmembrane cargoes. Thus, densely packed prebudding complex clusters induced by Sec13/31p might form a structural barrier for the incorporation of non-cargo proteins into the COPII vesicles. Although further investigation is necessary to clarify the precise mechanism, our study supports the assumption that the COPII components are required to mediate the exclusion of non-cargo proteins from COPII vesicles.

The minimal model we have presented here was designed to capture the core features of COPII vesicle formation, and we have shown that the minimal set of COPII components is not only required to collect cargo molecules, but also to facilitate exclusion of non-cargo proteins from the cargo clusters. The successful reconstitution of COPII-driven vesicle formation under a more physiologically relevant condition may increase the efficiency of cargo loading and vesicle formation. Nevertheless, it is likely that even in a complex cellular environment, the core COPII proteins would exhibit a similar potential for catalysing cargo concentration and exclusion of non-cargo proteins. Our approach may be generally useful for studying biochemical events within the membrane that involve multiple protein interactions.

## Materials and methods

### Plasmid constructions

The coding sequence for Bet1p with an N-terminal Strep-tag was generated by PCR from pKSE165 (Sato and Nakano, 2005) and inserted into the *EcoRI*–*Bam*HI sites of pASK-IBA5 (IBA) to yield pKSE143. A single cysteine residue was introduced at the C-terminus of Bet1p on pKSE143 by PCR mutagenesis, which codes for 2Strep-Bet1p-Cys, yielding the plasmid pKSE271. Four cysteine residues were introduced at the C-terminus of Bet1p on pKSE143 by

PCR mutagenesis, which codes for 2Strep-Bet1p-4Cys, yielding the plasmid pKSE272. The N-terminal domain of Sec12p (residues 1–373, Sec12 $\Delta$ Alum) with an N-terminal Strep-tag was generated by PCR from pKSE176 (Sato and Nakano, 2005) and inserted into the *EcoRI*–*XhoI* sites of pASK-IBA2 (IBA), which codes for 2Strep-Sec12 $\Delta$ Alum, yielding the plasmid pKSE253. A unique cysteine residue at position 171 originally present in wild-type Sar1p was replaced by serine and a single cysteine residue was introduced at the C-terminus of GST–Sar1p-C171S by PCR mutagenesis, which codes for GST–Sar1p-C171S-Cys, yielding the plasmid pKSE264.

### Preparation of fluorescent proteins

2Strep-Bet1p-Cys, 2Strep-Bet1p-4Cys, and 2Strep-Sec12 $\Delta$ Alum were purified from *Escherichia coli* C43 (DE3) cells containing the respective plasmids as described earlier (Sato and Nakano, 2005). The purification of MBP-Ufe1p was described before (Sato and Nakano, 2004). Purified 2Strep-Bet1p-Cys, 2Strep-Bet1p-4Cys, and MBP-Ufe1p were reacted with Cy3-maleimide (GE Healthcare) or ATTO647N-maleimide (ATTO TEC) in 20 mM HEPES–KOH, pH 8.0, 160 mM KOAc, and 1.25% octylglucoside at 25°C in the presence of Tris-(2-carboxyethyl)phosphine hydrochloride to yield 2Strep-Bet1p-Cy3, 2Strep-Bet1p-4Cy3, and MBP-Ufe1p-ATTO647N, respectively. After 1 h incubation, unreacted excess dye was removed by a NAP-10 column (GE Healthcare) equilibrated with 20 mM HEPES–KOH, pH 6.8, 160 mM KOAc, 1.25% octylglucoside. The labelling efficiencies were 0.98 (dye/protein) for Bet1p-Cy3, 3.1 (dye/protein) for Bet1p-4Cy3, and 2.9 (dye/protein) for MBP-Ufe1p-ATTO647N. Sar1p-C171S-Cys was prepared from GST–Sar1p-C171S-Cys cleaved by thrombin. Sar1p-C171S-Cys was reacted with Cy3-maleimide in 20 mM HEPES–KOH, pH 7.4, 160 mM KOAc, 1 mM MgOAc, and 0.005% Triton X-100 at 25°C in the presence of Tris-(2-carboxyethyl)phosphine hydrochloride to yield Sar1p-Cy3. After 1 h incubation, unreacted excess Cy3 dye was removed by a NAP-10 column (GE Healthcare) equilibrated with 20 mM HEPES–KOH, pH 6.8, 160 mM KOAc, 1 mM MgOAc, and 0.005% Triton X-100. The labelling efficiency was 0.73 (dye/protein).

### Preparation of proteoliposomes

Proteoliposomes were prepared from the major–minor mix lipid formulation as described (Sato and Nakano, 2005) except that the Ca<sup>2+</sup>-induced fusion step was omitted.

### Formation of horizontal lipid bilayers and protein incorporation

Artificial lipid bilayers were formed horizontally by placing the major–minor lipid mix dissolved in squalene or n-decane at the hole of the home-made upper chamber as described earlier (Ide and Yanagida, 1999). Membrane thickness was determined by measuring the capacitance of the bilayer as described before (White, 1970). Proteoliposomes reconstituted separately with 2Strep-Sec12 $\Delta$ Alum (170  $\mu$ g protein per ml<sup>-1</sup>, 1.8 mg lipid per ml<sup>-1</sup>), 2Strep-Bet1p-Cy3 (240  $\mu$ g protein per ml<sup>-1</sup>, 0.9 mg lipid per ml<sup>-1</sup>), 2Strep-Bet1p-4Cy3 (50  $\mu$ g protein per ml<sup>-1</sup>, 0.5 mg lipid per ml<sup>-1</sup>), or MBP-Ufe1p-ATTO647N (200  $\mu$ g protein per ml<sup>-1</sup>, 0.9 mg lipid per ml<sup>-1</sup>) were diluted with buffer (between 2- and 10 000-fold) containing 20 mM HEPES–KOH, pH 6.8, 150 mM KOAc, 2 mM MgCl<sub>2</sub>, 1% (v/v) glycerol, and 0.1 mM GTP or GMP-PNP, and added from the upper chamber onto the bilayer membrane, where they fused spontaneously with the bilayer membrane. After 10 min incubation to allow membrane fusion, excess proteoliposomes were withdrawn by a glass pipette. As ~90% of the N-terminal elements of the Bet1p-Cy3 were oriented on the outside of the liposomes (Sato and Nakano, 2005), an equal proportion of these regions of the bilayer-reconstituted Bet1p-Cy3 should be exposed to the upper surface of the bilayer membrane.

### Microscopy

The fluorescently labelled proteins in the artificial lipid bilayer were observed at room temperature with an objective-type total internal reflection fluorescence microscope that was constructed on an inverted research microscope (IX71, Olympus, Tokyo, Japan). An oil immersion objective lens (PlanApo, X60, 1.45 NA, Olympus) was located just below the lower chamber. Bilayers were illuminated either by evanescent wave or epifluorescence with a 532 nm Nd:YAG laser (COMPASS 315M-100, Coherent, Santa Clara, CA, USA) or a 632.8 nm He/Ne laser (05-LHP-151, Melles Griot, Carlsbad, CA, USA) according to the method of Tokunaga *et al* (1997).

In double-labelling experiments, sequential scanning was used to avoid any crosstalk of fluorescence channels. Images were recorded using an electron multiplying charge coupled device (iXon, DV887 DSC-DV, Andor, Belfast, Northern Ireland) and stored on a Windows PC. Video sequences were imported and analysed by Andor iQ software.

### Observation of fluorescently labelled molecules in the bilayer membrane

All experiments were performed at room temperature. To study the Bet1p-Cy3 assembly as shown in Figures 2A and 3, COPII components (~10 µl of the mixture containing 70 ng Sar1p, 410 ng Sec23/24p, and 1.4 µg Sec13/31p) were added from the upper chamber (total ~300 µl) to the bilayer membrane formed in an aqueous environment reconstituted with 2Strep-Bet1p-Cy3 and 2Strep-Sec12Δlum. The chamber solution contained 20 mM HEPES-KOH, pH 6.8, 150 mM KOAc, 2 mM MgCl<sub>2</sub>, and 0.1 mM GTP or GMP-PNP. Images were taken at a rate of 66 ms per frame. To study the Ufe1p-Cy3 dynamics shown in Figure 4, COPII components were added as above to the bilayer membrane reconstituted with MBP-Ufe1p-ATTO647N, 2Strep-Sec12Δlum, and 2Strep-Bet1p. In the downward budding experiments (Figure 2C), COPII components (~100 µl of the mixture containing 350 ng Sar1p, 2 µg Sec23/24p, and 7 µg Sec13/31p) were added to the bilayer membrane reconstituted with 2Strep-Bet1p-4Cy3 and 2Strep-Sec12-Δlum from the lower chamber, and at the indicated time points after the addition of COPII components, the fluorescent particles that appeared during the 10 s period on the surface of the coverslip were counted. Results were shown as the increase in the number of fluorescent particles relative to the initial number of fluorescent particles, which is defined as 100%. Images were taken at a rate of 66 ms per frame. For the measurements shown in Figure 1, COPII component(s) (~10 µl of the mixture containing 70 ng Sar1p, 410 ng Sec23/24p, and 1.4 µg Sec13/31p) were applied to the bilayer membrane formed in an aqueous environment, except for Figures 1F and G, where COPII components were added onto the bilayer formed on the coverslip and the following procedures described below were omitted. After a 5 min incubation to allow COPII binding, 10 µl of 1 µM annexin V (BioVison Research Products, Mountain View, CA, USA) was further added to the upper chamber

to immobilize the Bet1p-Cy3 proteins in the bilayer membrane as described before (Ide and Yanagida, 1999), and then the bilayer membrane was positioned down onto the coverslip followed by the measurements. In these cases, the chamber solution contained 2 mM CaCl<sub>2</sub> and 30% of dioleoylphosphatidylserine was further included in the bilayer membrane to allow annexin V binding, which decreases the lateral diffusion movement of Bet1p-Cy3. Images were taken at a rate of 66 ms per frame. Lateral diffusion constants were calculated before the addition of annexin V according to Ichikawa *et al* (2006). For the data analyses shown in Figure 1, the fluorescence intensities derived from a single Cy3 dye molecule showing single-step bleaching were averaged for 450–800 molecules (the range of the averaged intensity was from 1714 to 3281) and used to normalize the signal intensity of each dot. The histograms of Figure 1 were fitted to a Gaussian curve or the sum of two Gaussian curves  $y = A \cdot \exp(-(x-B)^2/C^2)$ , where the parameter *A* is the height of the peak, *B* is the centre value, and *C* is the width of the peak.

### Supplementary data

Supplementary data are available at *The EMBO Journal* Online (<http://www.embojournal.org>).

### Acknowledgements

We thank Toshio Yanagida for assistance with learning the planar bilayer microscopy. This work was supported by a grant-in-aid from the Ministry of Education, Culture, Sports, Science, and Technology of Japan (HN and KS) and a grant-in-aid for Scientific Research of the JSPS (KS), partly by the Targeted Proteins Research Program from MEXT (KS), and partly by the PROBRAIN (HN). This work was also supported by the fund from the Bioarchitect Project of RIKEN (KS).

### Conflict of interest

The authors declare that they have no conflict of interest.

### References

- Antonny B, Madden D, Hamamoto S, Orci L, Schekman R (2001) Dynamics of the COPII coat with GTP and stable analogues. *Nat Cell Biol* **3**: 531–537
- Barlowe C, Orci L, Yeung T, Hosobuchi M, Hamamoto S, Salama N, Rexach MF, Ravazzola M, Amherdt M, Schekman R (1994) COPII: a membrane coat formed by Sec proteins that drive vesicle budding from the endoplasmic reticulum. *Cell* **77**: 895–907
- Barlowe C, Schekman R (1993) SEC12 encodes a guanine-nucleotide-exchange factor essential for transport vesicle budding from the ER. *Nature* **365**: 347–349
- Bi X, Corpina RA, Goldberg J (2002) Structure of the Sec23/24-Sar1 pre-budding complex of the COPII vesicle coat. *Nature* **419**: 271–277
- Bielli A, Haney CJ, Gabreski G, Watkins SC, Bannykh SI, Aridor M (2005) Regulation of Sar1 NH2 terminus by GTP binding and hydrolysis promotes membrane deformation to control COPII vesicle fission. *J Cell Biol* **171**: 919–924
- Bonifacino JS, Glick BS (2004) The mechanisms of vesicle budding and fusion. *Cell* **116**: 153–166
- Bonifacino JS, Lippincott-Schwartz J (2003) Coat proteins: shaping membrane transport. *Nat Rev Mol Cell Biol* **4**: 409–414
- Fath S, Mancias JD, Bi X, Goldberg J (2007) Structure and organization of coat proteins in the COPII cage. *Cell* **129**: 1325–1336
- Fromme JC, Ravazzola M, Hamamoto S, Al-Balwi M, Eyaid W, Boyadjiev SA, Cosson P, Schekman R, Orci L (2007) The genetic basis of a craniofacial disease provides insight into COPII coat assembly. *Dev Cell* **13**: 623–634
- Futai E, Hamamoto S, Orci L, Schekman R (2004) GTP/GDP exchange by Sec12p enables COPII vesicle bud formation on synthetic liposomes. *EMBO J* **23**: 4146–4155
- Gimeno RE, Espenshade P, Kaiser CA (1996) COPII coat subunit interactions: Sec24p and Sec23p bind to adjacent regions of Sec16p. *Mol Biol Cell* **7**: 1815–1823
- Heinzer S, Worz S, Kalla C, Rohr K, Weiss M (2008) A model for the self-organization of exit sites in the endoplasmic reticulum. *J Cell Sci* **121**(Pt 1): 55–64
- Huang M, Weissman JT, Beraud-Dufour S, Luan P, Wang C, Chen W, Aridor M, Wilson IA, Balch WE (2001) Crystal structure of Sar1-GDP at 1.7 Å resolution and the role of the NH2 terminus in ER export. *J Cell Biol* **155**: 937–948
- Ichikawa T, Aoki T, Takeuchi Y, Yanagida T, Ide T (2006) Immobilizing single lipid and channel molecules in artificial lipid bilayers with annexin A5. *Langmuir* **22**: 6302–6307
- Ide T, Takeuchi Y, Aoki T, Yanagida T (2002) Simultaneous optical and electrical recording of a single ion-channel. *Jpn J Physiol* **52**: 429–434
- Ide T, Yanagida T (1999) An artificial lipid bilayer formed on an agarose-coated glass for simultaneous electrical and optical measurement of single ion channels. *Biochem Biophys Res Commun* **265**: 595–599
- Kirchhausen T (2000) Three ways to make a vesicle. *Nat Rev Mol Cell Biol* **1**: 187–198
- Kuehn MJ, Herrmann JM, Schekman R (1998) COPII-cargo interactions direct protein sorting into ER-derived transport vesicles. *Nature* **391**: 187–190
- Lee MC, Miller EA, Goldberg J, Orci L, Schekman R (2004) Bidirectional protein transport between the ER and Golgi. *Annu Rev Cell Dev Biol* **20**: 87–123
- Lee MC, Orci L, Hamamoto S, Futai E, Ravazzola M, Schekman R (2005) Sar1p N-terminal helix initiates membrane curvature and completes the fission of a COPII vesicle. *Cell* **122**: 605–617
- Matsuoka K, Orci L, Amherdt M, Bednarek SY, Hamamoto S, Schekman R, Yeung T (1998) COPII-coated vesicle formation reconstituted with purified coat proteins and chemically defined liposomes. *Cell* **93**: 263–275

- Miller EA, Beilharz TH, Malkus PN, Lee MC, Hamamoto S, Orci L, Schekman R (2003) Multiple cargo binding sites on the COPII subunit Sec24p ensure capture of diverse membrane proteins into transport vesicles. *Cell* **114**: 497–509
- Mossesso E, Bickford LC, Goldberg J (2003) SNARE selectivity of the COPII coat. *Cell* **114**: 483–495
- Nakano A, Muramatsu M (1989) A novel GTP-binding protein, Sar1p, is involved in transport from the endoplasmic reticulum to the Golgi apparatus. *J Cell Biol* **109**(6 Pt 1): 2677–2691
- Sato K, Nakano A (2004) Reconstitution of coat protein complex II (COPII) vesicle formation from cargo-reconstituted proteoliposomes reveals the potential role of GTP hydrolysis by Sar1p in protein sorting. *J Biol Chem* **279**: 1330–1335
- Sato K, Nakano A (2005) Dissection of COPII subunit-cargo assembly and disassembly kinetics during Sar1p-GTP hydrolysis. *Nat Struct Mol Biol* **12**: 167–174
- Sato K, Nakano A (2007) Mechanisms of COPII vesicle formation and protein sorting. *FEBS Lett* **581**: 2076–2082
- Springer S, Schekman R (1998) Nucleation of COPII vesicular coat complex by endoplasmic reticulum to Golgi vesicle SNAREs. *Science* **281**: 698–700
- Stagg SM, Gurkan C, Fowler DM, LaPointe P, Foss TR, Potter CS, Carragher B, Balch WE (2006) Structure of the Sec13/31 COPII coat cage. *Nature* **439**: 234–238
- Stagg SM, LaPointe P, Razvi A, Gurkan C, Potter CS, Carragher B, Balch WE (2008) Structural basis for cargo regulation of COPII coat assembly. *Cell* **134**: 474–484
- Stephens DJ, Pepperkok R (2004) Differential effects of a GTP-restricted mutant of Sar1p on segregation of cargo during export from the endoplasmic reticulum. *J Cell Sci* **117**(Pt 16): 3635–3644
- Supek F, Madden DT, Hamamoto S, Orci L, Schekman R (2002) Sec16p potentiates the action of COPII proteins to bud transport vesicles. *J Cell Biol* **158**: 1029–1038
- Tokunaga M, Kitamura K, Saito K, Iwane AH, Yanagida T (1997) Single molecule imaging of fluorophores and enzymatic reactions achieved by objective-type total internal reflection fluorescence microscopy. *Biochem Biophys Res Commun* **235**: 47–53
- Townley AK, Feng Y, Schmidt K, Carter DA, Porter R, Verkade P, Stephens DJ (2008) Efficient coupling of Sec23–Sec24 to Sec13–Sec31 drives COPII-dependent collagen secretion and is essential for normal craniofacial development. *J Cell Sci* **121** (Pt 18): 3025–3034
- White SH (1970) A study of lipid bilayer membrane stability using precise measurements of specific capacitance. *Biophys J* **10**: 1127–1148
- Yoshihisa T, Barlowe C, Schekman R (1993) Requirement for a GTPase-activating protein in vesicle budding from the endoplasmic reticulum. *Science* **259**: 1466–1468